



The Krüppel-like factor Cabut has cell cycle regulatory properties similar to E2F1

Peng Zhang^{a,b,1}, Alexia J. Katzaroff^{c,d,1}, Laura A. Buttitta^d, Yiqin Ma^{a,b}, Huaqi Jiang^d, Derek W. Nickerson^d, Jan Inge Øvrebø^{a,b}, and Bruce A. Edgar^{a,b,d,2}

^aHuntsman Cancer Institute, University of Utah, Salt Lake City, UT 84112; ^bDepartment of Oncological Sciences, University of Utah, Salt Lake City, UT 84112; ^cMolecular and Cellular Biology Program, University of Washington, Seattle, WA 98195; and ^dDivision of Basic Sciences, Fred Hutchinson Cancer Research Center, Seattle, WA 98109

Edited by Utpal Banerjee, University of California, Los Angeles, CA, and approved January 6, 2021 (received for review July 27, 2020)

Using a gain-of-function screen in *Drosophila*, we identified the Krüppel-like factor Cabut (Cbt) as a positive regulator of cell cycle gene expression and cell proliferation. Enforced *cbt* expression is sufficient to induce an extra cell division in the differentiating fly wing or eye, and also promotes intestinal stem cell divisions in the adult gut. Although inappropriate cell proliferation also results from forced expression of the *E2f1* transcription factor or its target, *Cyclin E*, Cbt does not increase E2F1 or Cyclin E activity. Instead, Cbt regulates a large set of E2F1 target genes independently of E2F1, and our data suggest that Cbt acts via distinct binding sites in target gene promoters. Although Cbt was not required for cell proliferation during wing or eye development, Cbt is required for normal intestinal stem cell divisions in the midgut, which expresses E2F1 at relatively low levels. The E2F1-like functions of Cbt identify a distinct mechanism for cell cycle regulation that may be important in certain normal cell cycles, or in cells that cycle inappropriately, such as cancer cells.

Cabut (Cbt) | cell cycle exit | E2F1 | intestinal stem cell (ISC) | proliferation

Accurate control of cell proliferation is important for the generation of properly sized and organized tissues and organs during development, and to maintain homeostasis during tissue maintenance in adults. Exit from the cell cycle is regulated such that cells typically exit into G1 upon terminal differentiation. Loss of this coordination or reversal of cell cycle exit can result in tissue dysplasia, developmental defects, and diseases such as cancer. Work in many systems investigating the role of negative regulators of G1 during cell cycle exit has demonstrated that members of the retinoblastoma (Rb) family of tumor suppressors and cyclin-dependent kinase inhibitors (CKIs) are required for cell cycle exit in some cell types, but are not required in others (1–4). Research focused on positive regulators of the cell cycle and has shown that the inhibition of the E2F1/dimerization partners (DP) transcription factors and G1 cyclin/cyclin-dependent kinase (Cdk) activities are key events in proper cell cycle exit (5–12). Recent studies also highlight the role of chromatin modification in establishing the postmitotic state during cell differentiation (13–15). Given that Rb and CKI family genes are not uniformly required for cell cycle exit, some of the mechanisms by which E2F1/DP and cyclin/Cdk activities are controlled upon exit remain unknown.

Most cell types in higher animals normally exit the cell cycle in G1, implicating the inhibition of S phase entry as the key regulated step. In eukaryotic cells, G1 to S phase progression is promoted by activating E2F transcription factors and their DPs. E2F/DP complexes control the expression of genes required for cell cycle progression, such as those involved in DNA replication and mitosis (16–20). The specific E2F subunit incorporated into a complex determines its function as either a transcriptional activator or constitutive repressor. Activating E2F complexes can also be converted to repressors when bound by Rb proteins (21, 22), and this association is lost upon the phosphorylation of the Rb proteins by either Cyclin D (CycD)/Cdk4 or Cyclin E (CycE)/

Cdk2 (23, 24). CKIs also participate in this regulation. CycE activity is restrained by members the Cip/Kip family of CKIs (p21, p27, and p57), while CycD activity is restrained by Ink-type CKIs (p15, p16, p18, and p19) (4, 12, 25, 26). Nevertheless, as CycE is a canonical transcriptional target of the activating E2Fs (E2F1, -2, -3), the E2F–CycE–RB interaction can generate a positive feedback loop for G1/S progression (27, 28), and this loop must be broken to allow exit into G1 phase.

Drosophila has been a key model organism for studying the cell cycle, in part because the fly genome contains fewer copies of cell cycle regulatory genes than mammalian genomes. *Drosophila* have one activating E2F (*E2f1*), one repressive E2F (*E2f2*), and a single DP gene (*Dp*), while humans have eight known E2Fs and three DP genes (8, 29–32). Furthermore, *Drosophila* have only two Rb genes (*Rbf*, *Rbf2*) (21), a single Cyclin D gene (*CycD*) (33), a single Cyclin E gene (*CycE*) (34), a single Cip/Kip-type CKI, Dacapo (*dap*) (30, 35, 36), and no Ink-type CKI. Investigations of cell cycle exit in *Drosophila* have been facilitated by the remarkably synchronous timing of cell cycle exit in both the pupal eye and wing blade. In both organs, cells complete all divisions by 24 h after puparium formation (APF, at 25 °C) and nearly 100% of the cells exit the cell cycle with a G1 DNA content (6, 37–39).

Genetic studies in *Drosophila* demonstrate that the negative regulators Rbf, Rbf2, E2F2, and Dap are only partially responsible for promoting cell cycle exit, and play a more significant

Significance

We discovered that the *Drosophila* transcription factor, Cabut, an ortholog of human KLF-10 and KLF-11, is capable of trans-activating a large set of cell cycle genes that are also E2F1 targets. Thereby, Cabut can drive ectopic cell cycles in many *Drosophila* cell types. That Cabut has E2F-like activity is especially interesting when one considers that the E2Fs, which are the best characterized transcriptional regulators of the eukaryotic cell cycle, are not actually essential for cell cycle gene transcription or cell cycle progression. Hence, it is clear that other transcription factors must also regulate the transcription of the 300 to 400 genes necessary for DNA replication and mitosis. Cabut appears to be one these missing transcription factors that can complement E2F.

Author contributions: P.Z., A.J.K., and B.A.E. designed research; P.Z., A.J.K., L.A.B., Y.M., H.J., D.W.N., and J.I.Ø. performed research; P.Z. and A.J.K. contributed new reagents/analytic tools; P.Z., A.J.K., L.A.B., Y.M., and J.I.Ø. analyzed data; and P.Z., A.J.K., and B.A.E. wrote the paper.

The authors declare no competing interest.

This article is a PNAS Direct Submission.

Published under the PNAS license.

¹P.Z. and A.J.K. contributed equally to this work.

²To whom correspondence may be addressed. Email: bruce.edgar@hci.utah.edu.

This article contains supporting information online at <https://www.pnas.org/lookup/suppl/doi:10.1073/pnas.2015675118/-DCSupplemental>.

Published February 8, 2021.

role in cell cycle exit in the developing eye than in the developing wing (5, 10, 20, 40, 41). We previously investigated the ability of positive cell cycle regulators to bypass cell cycle exit and identified a double assurance mechanism that limits continued cycling in the fly eye and wing. This work demonstrated that overexpression of either E2F1 or CycE caused a single extra cell cycle, and that their activities are independently constrained for proper exit, in part by Rbf- and Dap-independent mechanisms (5). Follow-up studies described the relationship between E2F1 and CycE after cell cycle exit (20), and the dynamic changes in chromatin structure that occur during differentiation (13), but precisely how the cell cycle control apparatus is constrained to ensure exit into G1 is still poorly understood in this and other developmental contexts.

To further understand the events regulating cell cycle exit, we took a gain-of-function approach to identify genes that were capable of delaying cell cycle exit when overexpressed, potentially by increasing the activity of E2F1 and CycE. Using this approach, we identified the Sp/Krüppel-like factor (KLF) family transcription factor Cabut (*cbt*), also known as dTIEG (42), as a potent cell cycle activator capable of delaying cell cycle exit when overexpressed. As detailed below, *Cbt* causes ectopic proliferation not by activating E2F1 or CycE, but instead by virtue of having its own E2F1-like transcriptional activity.

Results

PCNA-miniwhite⁺: A Reporter to Detect Ectopic E2F1 Activity as Eye Color. To identify new regulators of cell cycle exit, we designed a screen that detects ectopic E2F1 activity and cellular proliferation in the eye after normal cell cycle exit. To do this we generated the *PCNA-miniwhite⁺* reporter gene, which fuses an E2F1-responsive fragment from the *proliferating cell nuclear antigen (PCNA)* promoter (43) to the *miniwhite⁺* protein coding sequence (Fig. 1A). The pheno-critical period for *white* gene activity is 24 to 48 h APF (44), a time when all cells in the pupal eye have normally exited the cell cycle and transcription from the *PCNA* promoter and most other E2F1 target genes decreases (5). *w⁻* flies carrying the *pBac[eCFP PCNA-miniwhite⁺]* reporter gene normally had pale yellow eye color, likely due to the perdurance of White protein produced prior to cell cycle exit. We expected that when the silencing of E2F1 activity was abrogated or delayed, the eye would maintain *PCNA* promoter activity after 24 h APF, resulting in sufficient expression of *white* during the pheno-critical time to generate orange or red eye color. We tested this by crossing *PCNA-miniwhite⁺* into several mutant backgrounds. Cells mutant for the ubiquitin-ligase *archipelago (ago)* maintain CycE activity, and consequently delay cell cycle exit (35) and the silencing of E2F1 transcriptional activity in the eye. Accordingly, *ago* mutant cells generated clonally in *w⁻* *PCNA-miniwhite⁺* eyes displayed red eye color (Fig. 1B). We

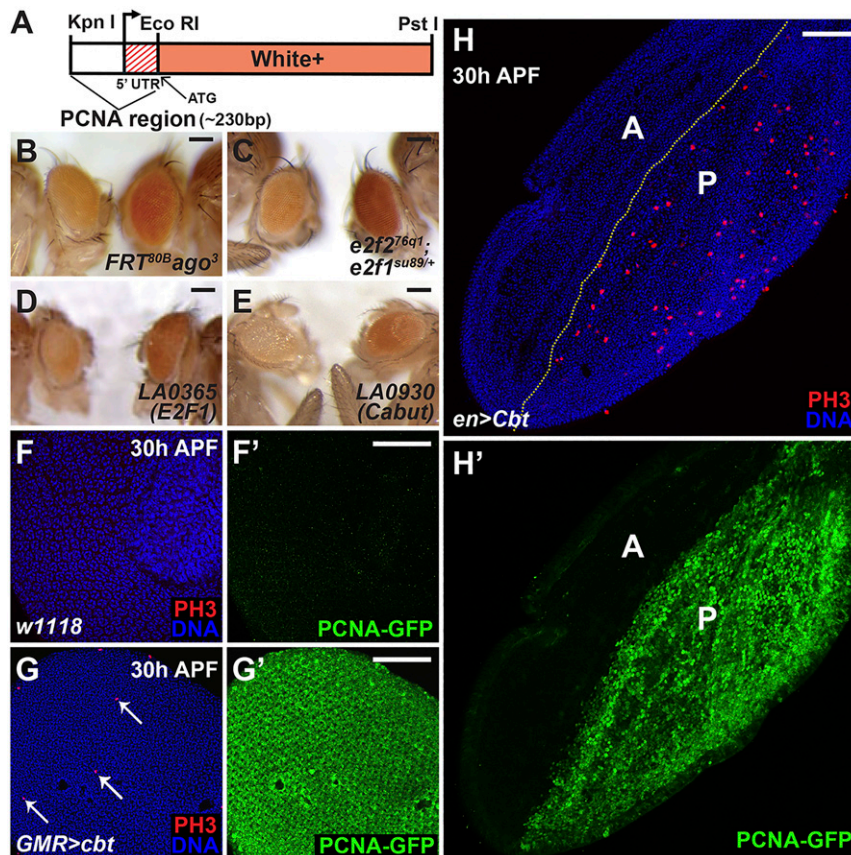


Fig. 1. A screen to identify regulators of the cell cycle identifies Cabut. (A) Schematic of the *PCNA-miniwhite⁺* reporter gene. (B–E) *Drosophila* carrying the *PCNA-miniwhite⁺* reporter and other transgenes or mutations, with age- and sex-matched controls on the left. (B) *FRT^{82B} ago³* mutant clones generated by *ey-FLP* have red eye pigmentation with *PCNA-miniwhite⁺*. (C) *e2f2^{76q1}; e2f1^{su89/+}* mutant eyes are red with *PCNA-miniwhite⁺*. (D and E) LA enhancer-promoter lines predicted to express either *E2f1* (LA0365) (D) or *cabut* (LA0930) (E) crossed to *GMR-Gal4(ey-CFP); PCNA-miniwhite⁺* (Right) have increased red eye pigmentation. (F) Thirty hours APF, control eyes did not undergo ectopic mitoses (anti-PH3 immunostaining, red) and showed no *PCNA-GFP* expression (F'). (G and H) Thirty hours APF, eyes and wings with *cbt* expression by *GMR-Gal4* and *en-Gal4*, respectively, demonstrated ectopic mitoses (red, G and H) and *PCNA-GFP* expression (green, G' and H'). Arrows in G indicated the mitotic (PH3⁺) cells. "A" and "P" shown in (H and H') marked the anterior and posterior compartments of the pupal wing. Nuclei were stained with Hoechst (blue) in F, G, and H. (Scale bars, 50 μm.)

also tested whether maintaining E2F1 activity by decreasing repressive E2F function could generate red eyes in *PCNA-miniwhite*⁺ flies. Thus, a single copy of the *e2f1*^{su89} allele, which is unable to bind Rbf (40), in an *E2f2*^{-/-} background also resulted in red eye color due to increased *PCNA-miniwhite*⁺ expression (Fig. 1C). We surmise that the *PCNA-miniwhite*⁺ gene can function as a reporter of ectopic E2F1 or CycE activity and cell proliferation.

Identification of Genes Causing Ectopic Proliferation. To identify genes involved in regulating cell cycle exit, we combined *PCNA-miniwhite*⁺ with *GMR-Gal4* marked by *ey-CFP* and screened the University of California, Los Angeles collection of unidirectional UAS element insertion lines (LA lines, from John Merriam, University of California, Los Angeles, CA). We screened 400 nonredundant lines, and obtained 15 positive hits with increased eye pigmentation (SI Appendix, Table S1). Included in these hits were lines predicted to overexpress *E2f1* (Fig. 1D) and *CycE*, demonstrating the ability of the approach to detect ectopic proliferation. Activation of *LA0930* by *GMR-Gal4* also caused red eye color when compared to age- and sex-matched sibling controls (Fig. 1E). The nearest downstream annotated gene to the mapped *LA0930* insertion site encodes the transcription factor Cbt, suggesting that *cbt* overexpression was responsible for activation of the *PCNA* promoter. Prior studies of Cbt had identified it as a member of the SP/KLF family of transcription factors. Cbt has been proposed to be involved in Decapentaplegic (Dpp) signaling during embryonic dorsal closure and in the larval wing disk (45–48), to associate with the Yorkie (Yki) transcription factor (49), and to coordinate energy metabolism during sugar sensing (50).

We confirmed that overexpressed *cbt* activated the *PCNA* promoter by analyzing the effect of a *UAS-cbt* transgene on another E2F1-responsive reporter, *PCNA-GFP* (43), which contains the same *PCNA* promoter fragment as *PCNA-miniwhite*⁺. *Cbt* expression controlled by *GMR-Gal4* resulted in ectopic *PCNA-GFP* expression at 30 h APF in the pupal eye (Fig. 1G'). *Cbt* expression in the posterior wing compartment, driven by *engrailed (en)-Gal4* also induced strong ectopic *PCNA-GFP* expression (Fig. 1H'), demonstrating that Cbt activates the *PCNA* promoter in multiple tissues.

Cbt Causes an Ectopic Cell Cycle. Immunostaining for phosphohistone H3 (PH3), a marker of mitosis, showed that ectopic Cbt not only promoted *PCNA* expression, but also triggered ectopic cell divisions in both the wing and eye at 30 h APF (Fig. 1 G

and H). To determine whether these ectopic mitoses represented complete extra cycles, we generated GFP-labeled clones using the *hs-flp; tub > CD2 > Gal4; tub-Gal80^{ts}* method, which allows the conditional expression of UAS-linked transgenes (51). Clones expressing *UAS-cbt* were generated 48 to 72 h after embryo deposition (AED), in animals raised at 18 °C to prevent Gal4-mediated expression. These animals were shifted to 29 °C at 0 h APF, thereby inactivating Gal80^{ts} and activating Gal4 and *UAS-cbt* expression. *Cbt* expression in clones caused ectopic mitoses, ectopic DNA replication visualized by EdU labeling (Fig. 2A and SI Appendix, Fig. S1 A and A') and ectopic S and G2 phases, as visualized by anti-Cyclin A (CycA) immunostaining (Fig. 2B and SI Appendix, Fig. S1 B and B') at time points after normal cell cycle exit. The presence of cells in different cell cycle phases in *cbt*-expressing clones indicated an induction of ectopic cell proliferation.

To further assess cell cycle phasing in *cbt* overexpressing cells, we used FACS to measure DNA content. In this case, we used *apterous (ap)-Gal4 tub-Gal80^{ts}* to induce *UAS-GFP* and *UAS-cbt* in the dorsal wing blade at 0 h APF, while the ventral wing blade served as a GFP⁻ wild-type control. At 30 h APF, a significant proportion of GFP⁺ *cbt*-expressing cells were present in S and G2 phases, while essentially all wild-type non-GFP-expressing cells had exited the cell cycle into G1 phase (Fig. 2C). We also analyzed pupal eyes and wings expressing *cbt* at 44 h APF. We did not see ectopic mitoses or DNA replication at this timepoint, indicating that cell cycle exit had occurred prior. However, FACS analysis at 44 h APF showed that many *cbt* expressing cells still had a G2 DNA content (Fig. 2D). Given that no DNA replication was seen in *cbt*-expressing cells after 36 h APF, our results indicate that Cbt induced a single ectopic S phase in a large proportion of cells, followed by an ectopic M phase in a smaller proportion.

Another possible explanation for the phenotype observed upon *cbt* overexpression is a developmental delay, such that cells divide the appropriate number of times but do so more slowly than in the wild-type, consequently cycling longer into the pupal stage. To address this possibility, we used clonal labeling to count the number of cell divisions in pupal wings (5). Using the *hs-flp; tub > CD2 > Gal4; tub-Gal80^{ts}* system, labeled clones were generated at 0 h APF and wings were dissected and fixed between 40 and 44 h APF. More than 100 clones per genotype were scored. GFP⁺ control clones contained on average 2.33 ± 0.07 cells per clone, illustrating the single cell division that occurs between 0 and 24 h APF. Clones expressing *cbt* contained an

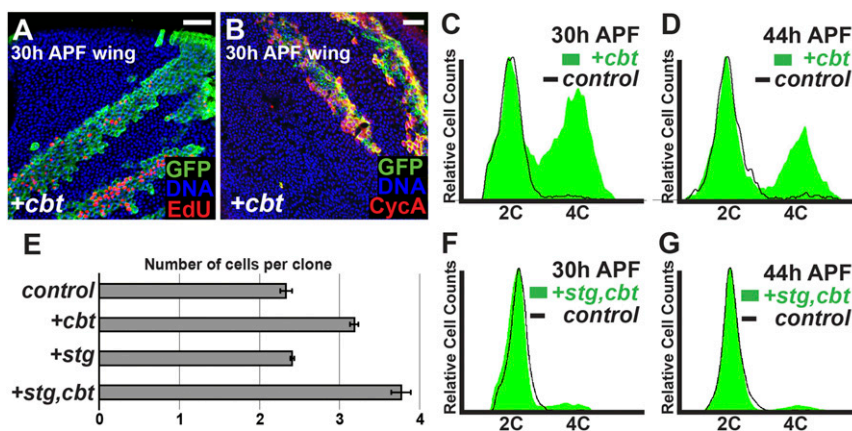


Fig. 2. Cbt causes an ectopic cell cycle in pupal wings. (A and B) Thirty hours APF, wings with GFP⁺-marked clones (green) expressing *cbt* by *hs-flp; tub > CD2 > Gal4; tub-Gal80^{ts}*. Cbt induced ectopic DNA replication by EdU incorporation (red) and ectopic S and G2 phases by anti-CycA staining (red). Nuclei were stained with Hoechst (blue). (Scale bars, 20 μm.) (C, D, F, and G) FACS of *ap-Gal4; tub-Gal80^{ts}* wings with GFP labeled *cbt* expression (C and D) or *cbt+stg* coexpression (F and G) at 30 h APF (C and F) and 44 h APF (D and G). (E) Number of cells per clone for a given genotype, with clonal induction at 0 h APF.

average of 3.17 ± 0.05 cells per clone (Fig. 2E), consistent with our conclusion that overexpressed Cbt induced a single ectopic cell cycle in ~50% of cells.

Coexpression of String with Cbt Bypasses Exit into G2. A significant proportion of *cbt*-expressing cells exited the cell cycle with a G2 DNA content. One potential explanation for this is that Cbt activity cannot prevent the down-regulation of one of more factors involved in M phase progression, which occurs at 24 h APF in cells exiting the cell cycle normally. We addressed this possibility by coexpressing *cbt* with the M phase activator String (Stg), a Cdc25-type phosphatase that activates Cdk1 and triggers mitosis in most *Drosophila* cells (52–54). In 30-h APF wings, coexpression of *cbt* with *stg* resulted in a majority of cells with a G1 DNA content (Fig. 2F). Wings coexpressing *cbt* and *stg* at 44 h APF also contained fewer G2 cells than wings expressing *cbt* alone (Fig. 2D and G). These results suggest that the addition of *stg* to *cbt* overexpression allows a greater number of cells to complete an entire ectopic cell cycle prior to exiting the cell cycle. To confirm that ectopic cell divisions still occurred during *cbt*+*stg* coexpression, we generated GFP-labeled clones at 0 h APF and scored clone size at 40 to 44 h APF in pupal wings. While clones

expressing *cbt* alone contained an average of 3.17 ± 0.05 cells per clone, clones coexpressing *cbt* and *stg* contained an average of 3.77 ± 0.12 (Fig. 2E). This suggests that although *cbt* is able to induce ectopic proliferation, it does so without inducing sufficient amounts of Stg activity to drive all cells through an extra cycle.

Cbt Promotes G1/S Progression in Proliferating Cells. To better understand the effects of Cbt as a cell cycle regulator, we analyzed the effect of *cbt* overexpression in proliferating cells. GFP-labeled *cbt*-expressing clones were induced using the *hs-flp;act > CD2 > Gal4* system at 48 h AED, and clones were analyzed 72 h later in the third-larval instar wing discs, when most cells still proliferate. FACS analysis showed that *cbt* expressing cells were slightly more likely to be in G2 phase than control cells, further indicating a role for Cbt in G1/S progression (Fig. 3A). When we analyzed these clones to determine if *cbt* expression affected the number of cell divisions, we found that there was no significant effect on the number of cells per clone (Fig. 3B). These data indicate that *cbt* overexpression promotes G1/S in proliferating wing cells without affecting overall cell doubling times. This is consistent with the effects of other positive G1/S regulators in

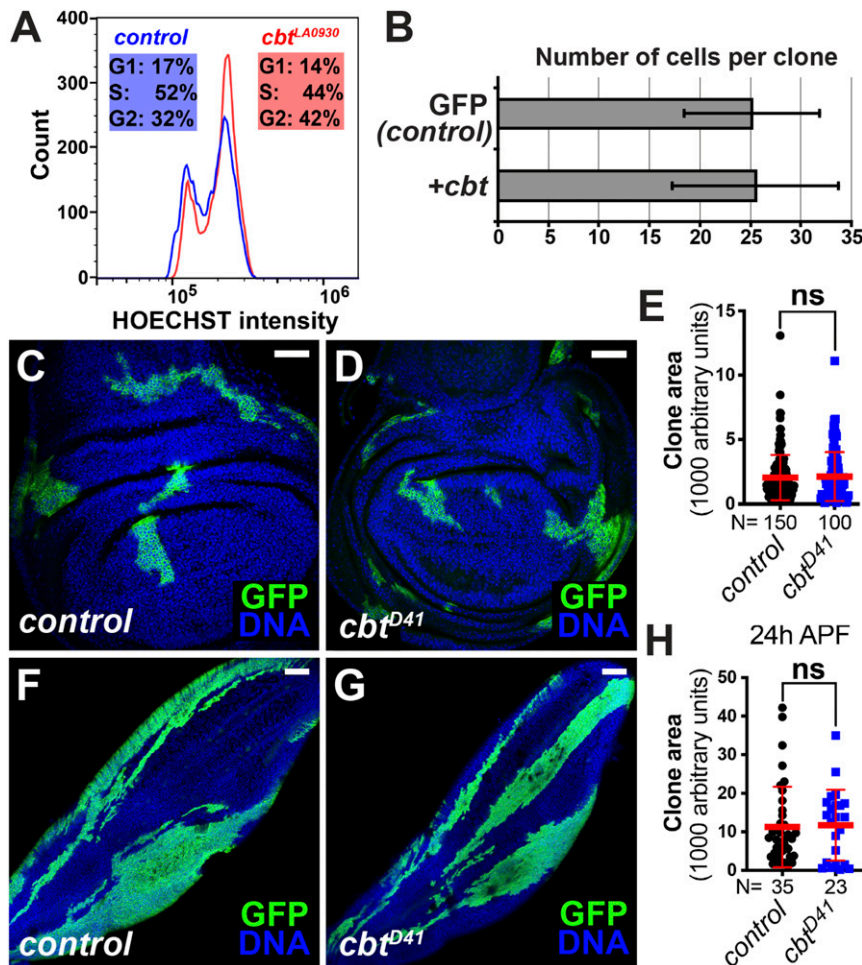


Fig. 3. Cbt promotes G1/S progression in proliferating cells. (A and B) GFP⁺-labeled clones (green) expressing *cbt* were induced at 48 h AED by *hs-flp;act > CD2 > Gal4* and analyzed at the third-larval instar. (A) Cells expressing *cbt* (*cbt^{LA0930}*) were shifted from G1 and S phase to G2, relative to GFP⁻ control cells. Cell counts per experiment were ~10,000. Samples were run on a Cytoflex flow cytometer. (B) *cbt* expression (*UAS-cbt*) did not cause an increase number of cells per clone compared to wild-type controls. (C–H) *cbt^{D41/D41}* mutant clones were generated by MARCM system at 48 h AED and analyzed in the third-instar wing discs (C–E) or 24-h APF wings (F–H). Representative images showed the clone areas of wild-type control (C and F) and *cbt^{D41/D41}* mutant (D and G). Clones were labeled by GFP. Nuclei were stained with DAPI (blue). (E and H) Quantification of MARCM clone areas (mean \pm SD, *t* test, nonsignificant [ns] $P > 0.05$). Each dot represents one sample. (Scale bars, 40 μ m in C and D; 80 μ m in F and G.)

the wing, like Cyclin E, which can accelerate G1/S progression without affecting the overall number of cell cycles (55).

Cbt Is Dispensable for Wing Cell Proliferation. Next, we asked whether the loss of *cbt* function caused a proliferative defect in cycling cells. To address this question, we required a null *cbt* mutant. However, all of the available deletions that eliminate *cbt* also disrupt an adjacent gene, *Mediator complex subunit 15 (MED15)* (*SI Appendix, Fig. S2A*) (45). Given this, we generated two new *cbt* mutants, *cbt^{D41}* and *cbt^{D148}*, by P-element excision (*SI Appendix,*

Fig. S2A). Both alleles are small deletions within *cbt* that do not impinge on *MED15*. Using complementation tests, we determined that *cbt^{D41}* is a null *cbt* allele while *cbt^{D148}* is not (*SI Appendix, Fig. S2B*). Lethal phase tests showed that most homozygous *cbt^{D41/D41}* mutants died during the second-larval instar, and that ~5% survived past the third larval instar but died in the pupal stage (*SI Appendix, Fig. S2C*). Furthermore, by applying the Fly-FUCCI system (56), we found that the homozygous third-instar *cbt^{D41/D41}* larvae had small wing imaginal discs with disrupted cell cycle progression (*SI Appendix, Fig. S2D*), suggesting that Cbt is

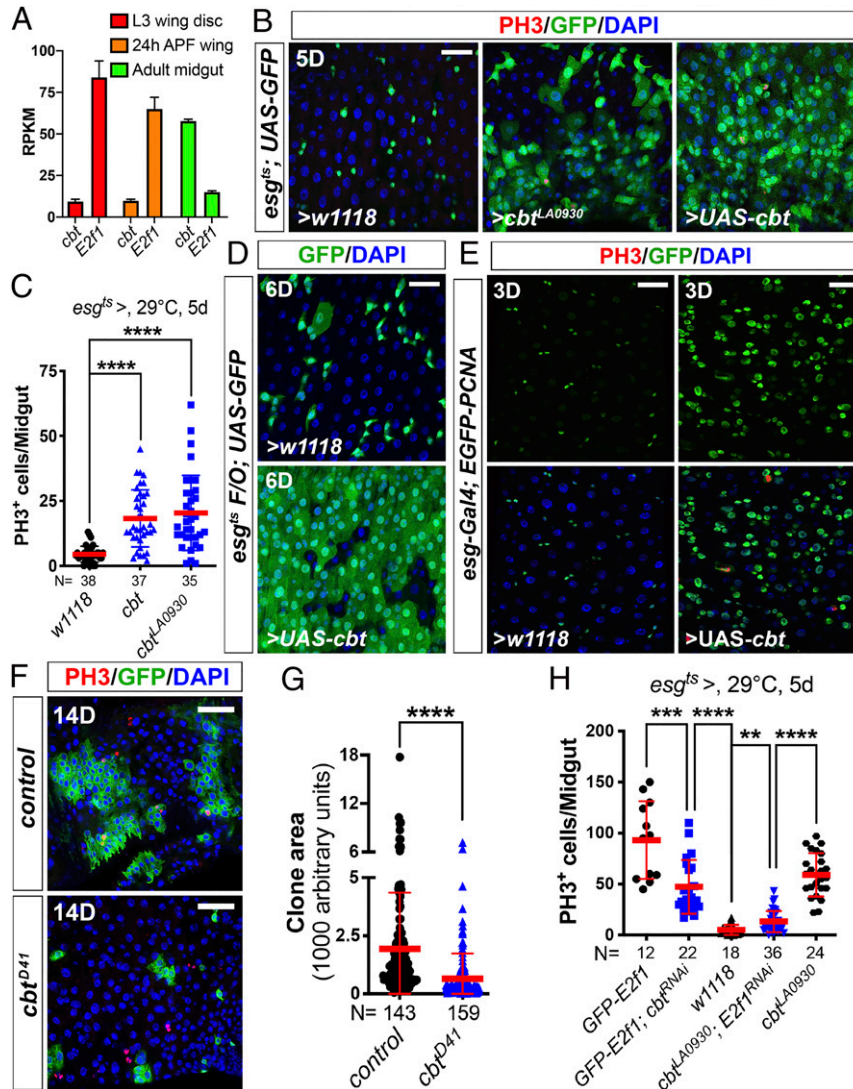


Fig. 4. Cbt compensates E2F1 for intestinal stem cell proliferation. (A and B) The expression levels of *cbt* and *E2f1* were checked using available RNA-seq datasets. The third-instar wing disc and pupal wing RNA-seq data (A) were published in Ma et al. (13). The midgut RNA-seq data (A) was generated in the B.A.E. laboratory. (B) Overexpression of *cbt* in progenitor cells was driven by *esg^{ts}*. Two- to 3-d-old adult females were shifted from 18 °C to 29 °C for 5 d before dissection. Midguts were stained with anti-GFP and anti-PH3 antibodies and DAPI. ISC mitoses were quantified by PH3⁺ cells. (Scale bar, 30 μm.) Quantification data shown in C represents the mean ± SD (t test, ****P < 0.0001). Each dot represents one sample. (D) *UAS-cbt* was overexpressed by the *esg^{ts} F/O* system. *Esg^{ts} F/O > w1118* was used as control. Flies were raised at 18 °C and then shifted to 29 °C for 6 d before dissection. Midguts were stained with anti-GFP antibody and DAPI. (Scale bar, 30 μm.) (E) Overexpression of *cbt* in progenitor cells driven by *esg-Gal4*. Flies were raised at 29 °C. 3-d-old adult females were dissected and stained with anti-GFP and anti-PH3 antibodies and DAPI. These pictures were taken from the R5 region of the midguts with the same laser settings on the confocal microscope. (Scale bars, 30 μm.) (F) *cbt^{D41/D41}* mutant clones were generated using the MARCM system. Representative images showed the clone areas of wild-type control (F, Upper) and *cbt^{D41/D41}* mutant (Lower) clones 14 d after clone induction. MARCM clones were labeled by GFP. Mitotic cells were stained with anti-PH3 antibody. Nuclei were stained with DAPI (blue). (Scale bars, 40 μm.) (G) Quantification of MARCM clone areas: control (n = 143 clones) versus *cbt^{D41/D41}* mutant (n = 159 clones) (mean ± SD, t test, ****P < 0.0001). (H) Different genetic manipulations in progenitor cells driven by *esg^{ts}*. Two- to 3-d-old adult females were shifted from 18 °C to 29 °C for 5 d before dissection. Midguts were stained with anti-GFP and anti-PH3 antibodies and DAPI. ISC mitoses were quantified by PH3⁺ cells. Quantification data represent the mean ± SD (t test, **P < 0.01, ***P < 0.001, ****P < 0.0001). Each dot represents one sample.

essential for normal tissue growth. To more accurately test whether Cbt is required for cell cycle progression in the wing, we performed mosaic analysis with a repressible cell marker (MARCM) clonal assays using the *cbt*^{D41/D41} allele. Cell clones homozygous for *cbt*^{D41} did not show growth defects in either third instar larval wing discs (Fig. 3 C–E) or pupal wings (Fig. 3 F–H). This indicates that, in wing development, other cell cycle regulators (e.g., E2F1) may compensate for Cbt's function in G1/S progression.

Cbt Regulates Intestinal Stem Cell Proliferation. Although our tests showed that Cbt is not required for cell cycle regulation in the developing wing, we suspected that its cell cycle regulatory functions could be important in other tissues. For example, Cbt could be less relevant for cell cycle progression in cell types that have high levels of E2F1, and more important in tissues that have relatively less E2F1. To test this idea, we compared the relative mRNA expression levels of *E2f1* and *cbt* between the wing and the adult midgut (intestine), a tissue that supports high levels of proliferation during epithelial regeneration. Using RNA-sequencing (RNA-seq) datasets from our laboratory and others (13), we found that *cbt* mRNA expression was much higher than *E2f1* in the adult midgut, whereas the reverse was true in larval and pupal wings (Fig. 4A). These expression patterns suggested that Cbt could be important for cell proliferation in the midgut.

Hence, we assessed *cbt* function in the adult midgut. Consistent with what we observed in the wing and eye, overexpression of *cbt* in midgut progenitor cells (intestinal stem cells [ISCs] and enteroblasts) using the *esg-Gal4 tub-Gal80^{ts} UAS-GFP (esg^{ts})* driver significantly increased ISC mitoses (Fig. 4 B and C). Using the *esg^{ts}F/O* system (*esg-Gal4 tubGal80^{ts} UAS-GFP act > CD2 > Gal4 UAS-flp*), which labels ISCs and all their clonal progeny after a temperature shift, we tested if *cbt* overexpression could influence gut epithelial turnover. Normally, the midgut epithelium renews in ~12 d at 29 °C in females (57). However, in the *cbt* overexpression condition, virtually complete gut renewal was achieved by 6 d (Fig. 4D), indicative of accelerated stem cell divisions.

Next, to assess whether ectopic Cbt-driven ISC proliferation is related to the regulation of cell cycle genes, we examined the expression of *PCNA* using an EGFP-tagged PCNA transgenic line (58). We found that overexpression of *cbt* in ISCs significantly increased the levels of *EGFP-PCNA* (Fig. 4E), suggesting that Cbt's ISC phenotypes are, at least in part, a result of the up-regulation of the cell cycle genes like PCNA. Furthermore, MARCM clonal analysis showed that *cbt*^{D41/D41} mutant clones grew significantly less than wild-type controls (Fig. 4 F and G). Thus, in contrast to the situation in the wing and eye, *cbt* is both limiting and required for normal ISC proliferation. To address the relationship of *cbt* to *E2f1* in the midgut, we performed genetic epistasis experiments using RNAi. We found that depletion of *E2f1* significantly repressed ISC mitoses driven by overexpressed *cbt* (Fig. 4H) and, conversely, that depletion of *cbt* also repressed E2F1-induced ISC proliferation (Fig. 4H). However, these repressive actions were not complete, suggesting a partial overlap of Cbt and E2F1 function.

Cbt and E2F1 Regulate a Shared Set of Cell Cycle Target Genes. To gain insight into how *cbt* regulates G1/S progression, we used oligonucleotide expression arrays to determine the how overexpressed *cbt* alters gene expression in developing wings. After 24 h of *cbt* overexpression, RNA samples were taken from proliferating wing cells (third-larval instar, L3), at the time of normal cell cycle exit (24 h APF), and after cell cycling had normally ceased (36 h APF). We identified 598 transcripts (SI Appendix, Table S2) affected by *cbt* expression with a fold-change of 1.3 or greater ($\log_2 \pm 0.4$ compared to controls, $P < 0.05$) compared to similarly staged control wings at both the 24-h and 36-h APF time points. We further compared the effects of *cbt* overexpression

to the effects of *E2f1/DP* overexpression at 24 h and 36 h APF (20). Overall, we observed a remarkable similarity between the transcript changes in *cbt*- and *E2f1/DP*-expressing wings. We took a conservative approach in our comparison by requiring that transcripts be affected by both Cbt and E2F1 with a fold-change of 1.3 or greater ($\log_2 \pm 0.4$ compared to controls, $P < 0.05$), at both 24 h and 36 h APF, to describe them as coregulated. Using this metric we identified 334 transcripts that were coregulated by both Cbt and E2F1. Many of these have previously been identified as E2F1 targets (16–19) (Fig. 5A). Comparison between Cbt- and E2F1-affected transcripts at 24 h APF gave a correlation coefficient of 0.43. There was a correlation coefficient of 0.57 between E2F1- and Cbt-affected transcripts at 36 h APF. Furthermore, comparison of transcripts affected at 24 h APF to those affected at 36 h APF gave a correlation coefficient of 0.39 ($P < 1e^{-6}$), indicative of similar regulatory actions of Cbt and E2F1. Analysis of enriched gene ontology (GO) terms among these transcripts yielded the terms “cell cycle” ($P < 5.28e^{-19}$), “chromosome segregation” ($P < 6.48e^{-11}$), and “cell division” ($P < 2.13e^{-10}$), further emphasizing the ability of Cbt to regulate the transcription of genes involved in cell cycle progression.

Cbt also regulated 279 transcripts that were not significantly regulated by E2F1 at both 24- and 36-h APF time points (Fig. 5B). These transcripts were not significantly enriched for any GO term and many of these genes are uncharacterized. This indicates that, although *cbt* can play a significant role in cell cycle progression, it likely has other functions unrelated to the cell cycle, as previously proposed (50, 59–62).

It should be noted that although ectopic *cbt* induced a significant number of genes known to be E2F1 targets, several well-validated E2F1 targets were not activated (Fig. 5C). Included in this group were *cycE* and *stg*, the rate-limiting factors for S and M phase progression in the wing, respectively (55, 63). This is consistent with the results we obtained by *cbt* and *stg* coexpression (Fig. 2 E–G). To confirm that these transcripts were not affected by *cbt* overexpression at cell cycle exit, we did reverse-transcription quantitative PCR (RT-qPCR) on mRNA from wings expressing *cbt* under *ap-Gal4;tub-Gal80^{ts}* control at 30 h APF (Fig. 5D). In agreement with the microarray data, RT-qPCR showed that Cbt did not increase *cycE* or *stg* transcript levels, but that *pcna* and *mr-S* levels were significantly increased. These results demonstrate a role for Cbt in regulating the expression of genes involved in cell cycle progression, but not in controlling the G1/S and G2/M rate-limiting factors, *cycE* and *stg*.

Cbt Acts Independently of E2F1. We next assessed the relationship of Cbt and E2F1 in cell cycle progression. Although RT-qPCR data suggested that overexpressed *cbt* might promote *E2f1* expression (Fig. 5D), assays using an enhancer trap allele of *E2f1* (*E2f1^{MT29}*) that is commonly used as a reporter for transcription of the *E2f1* locus (64, 65) did not confirm this (SI Appendix, Fig. S3 A and A'). To analyze the effect of *cbt* on E2F1 protein levels, GFP-labeled overexpression clones were generated and analyzed at 27 h APF using immunofluorescence with an anti-E2F1 antibody. In both wings and eyes, clones overexpressing *E2f1* had very high E2F1 protein levels (Fig. 5 E and E' and SI Appendix, Fig. S3 B and B'), but *cbt* overexpression did not increase the expression E2F1 protein (Fig. 5 F and F' and SI Appendix, Fig. S3 C and C'). To further test whether E2F1 levels were altered in the loss-of-function clones of *cbt*, we performed MARCM clonal assays using the *cbt*^{D41/D41} allele. Cell clones homozygous for *cbt*^{D41} did not show any alteration of E2F1 protein levels in third-instar wing or eye discs (SI Appendix, Fig. S3 D–E'). These observations indicate that ectopic *cbt* promotes cell cycle progression without increasing *E2f1* mRNA or protein expression.

Next, to further explore the relationship between *cbt* and *E2f1* target genes, we carried out de novo motif discovery on our microarray data using Multiple Em for Motif Elicitation (MEME,

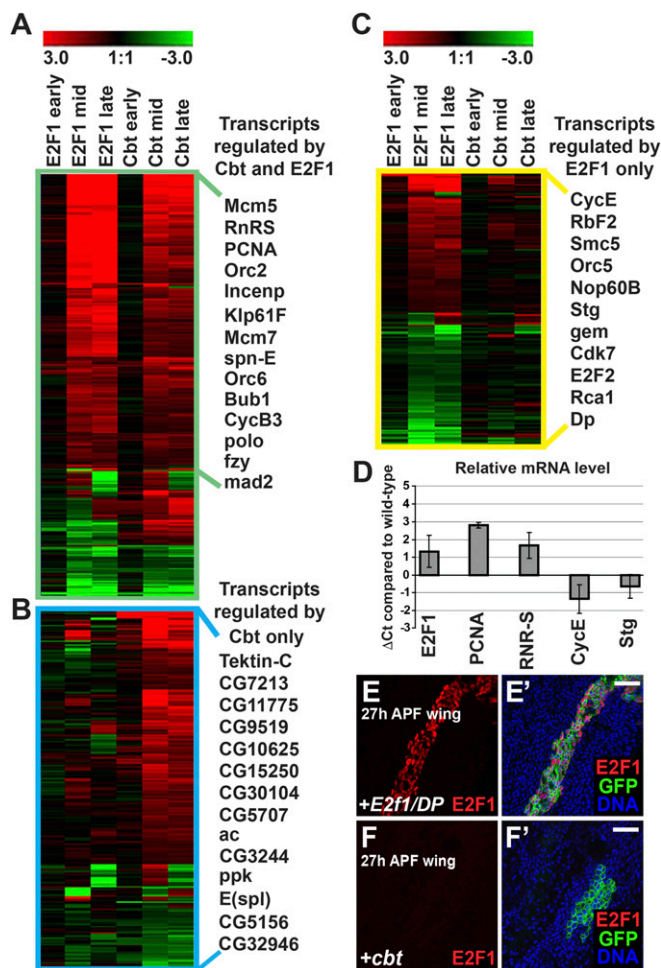


Fig. 5. Cbt and E2F1 regulate a shared set of cell cycle genes. (A–C) Microarray analysis of gene expression in *cbt* or *E2f1/DP* expressing wings by *ap-Gal4; tub-Gal80^{ts}* compared to controls (*y, w, hs-flp*). Heatmaps show transcript changes (color range indicates the \log_2 ratio of expression compares to controls). Transcripts were hierarchically clustered using Genesis software and with representative transcripts to the right. (A) Heatmap of the 334 transcripts significantly regulated by both E2F1/DP and Cbt. All transcripts with a fold-change of 1.3 or more ($\log_2 \pm 0.4$, $P < 0.05$) at both 24 h (mid) and 36 h (late) APF time points are shown. (B) Heatmap of the 279 transcripts regulated by Cbt with a fold-change of 1.3 or more ($\log_2 \pm 0.4$, $P < 0.05$) at both time points but not by E2F1/DP. (C) Heatmap of 200 of the >2,000 transcripts regulated by E2F1/DP with a fold-change of 1.3 or more ($\log_2 \pm 0.4$) but not by Cbt at both time points. (D) RT-qPCR quantification of gene expression in wings expressing *cbt* compared to controls. Cbt was induced at 0 h APF by *ap-Gal4; tub-Gal80^{ts}* and levels of transcript expression at 30 h APF was quantified by the $\Delta\Delta Ct$ method (97). Wild-type expression at 30 h APF is equivalent to 0Ct while comparative changes in transcript level in *cbt* expressing wings was measured by ΔCt , equivalent to the \log_2 of the difference in transcript level. ΔCt values represent the average of three biological replicates and error bars demonstrate the range. (E–F) GFP marked clones generated by *hs-flp; tub > Gal4; tub-Gal80^{ts}* expressing *E2f1/DP* (E and E') or *cbt* (F and F') analyzed in 27-h APF wings. Overexpression of *E2f1/DP* strongly increased E2F1 protein detected by immunofluorescence (red), whereas overexpression of *cbt* did not. Nuclei were counter stained with Hoechst 33258 (blue). (Scale bars, 20 μm .)

PMID: 19458158) (66). This work identified a putative regulatory motif, GCAGYKGCAGCG (SI Appendix, Fig. S4A), that is overrepresented in the promoters of many Cbt-regulated genes (E-value: 1.6e-014), as well as in the set of Cbt and E2F1 coregulated genes (E-value: 6.1e-004). To evaluate whether this

motif might be a Cbt-binding site, we used Cbt chromatin immunoprecipitation-sequencing (ChIP-seq) data from fly embryos from the modENCODE project (67), and carried out similar de novo motif discovery analysis of all Cbt binding regions. This identified a motif very similar to the one given by our own microarray data (SI Appendix, Fig. S4A). This further suggests that our analysis has identified true Cbt targets, and that GCAGYKGCAGCG is likely to be a Cbt binding site. As expected, this motif is present in the *PCNA* promoter (SI Appendix, Fig. S4B), consistent with the interpretation that *pcna* is a direct binding target of Cbt. In addition, to assess whether Cbt binding was observed in the promoters of the cell cycle genes that were activated by *cbt* overexpression, we examined the overlap of Cbt ChIP peaks published by Ruiz-Romero et al. (49) and the Cbt target genes from our microarray data (SI Appendix, Table S2). Both of these datasets were generated from wing discs. Among the 554 genes (598 transcripts) that were transcriptionally regulated by Cbt, 86 (including *PCNA*) had Cbt binding sites (SI Appendix, Table S3). These 86 overlapping genes define likely direct transcriptional targets of Cbt. GO analysis showed that most of these genes are cell cycle genes (SI Appendix, Table S4). These results further emphasize the ability of Cbt to regulate the transcription of genes involved in cell cycle progression.

To better understand how *cbt* functions related to *E2f1*, we investigated control of the *PCNA-GFP* reporter gene, which is often used to assay E2F1 activity (43). The two E2F1 binding sites in this reporter are not completely necessary for *pcna* transcription, as GFP is still weakly transcribed in a version of the reporter mutated in these two E2F1 binding sites ($\Delta PCNA-GFP$) (43). However, these E2F1 binding sites are required for high-level transcription in response to E2F1 in normal cells. Interestingly, ectopic expression of *cbt* in third-instar wing or eye discs activated $\Delta PCNA-GFP$ expression (Fig. 6 B and B' and SI Appendix, Fig. S5 B and B'), whereas ectopic *E2f1/DP* did not (Fig. 6 A and A' and SI Appendix, Fig. S5 A and A'). We also generated *cbt* or *E2f1/DP* overexpressing cell clones and analyzed these for $\Delta PCNA-GFP$ induction after cell cycle exit at 27 h and 44 h APF. In these cases as well, overexpressed *E2f1/DP* did not induce $\Delta PCNA-GFP$ (Fig. 6 C, C', E, and E' and SI Appendix, Fig. S5 C and C'), whereas overexpressed *cbt* did (Fig. 6 D, D', F, and F' and SI Appendix, Fig. S5 D and D'). Furthermore, we found that overexpression of dTIEG, the shorter isoform of Cbt that lacks 81 amino acids at the N terminus (SI Appendix, Figs. S2A and S6A), was unable to activate $\Delta PCNA-GFP$ in eye discs (SI Appendix, Fig. S6 B–C'). dTIEG could, however, activate the wild-type *PCNA-GFP* reporter (SI Appendix, Fig. S6 D–E'). These results indicate that Cbt can activate the expression of some E2F1 target genes (e.g., *pcna*) independently of E2F1 binding sites, and that this requires specific sequences in the *cbt* N terminus.

Cbt Drives Ectopic Proliferation Independently of Dp. Finally, we investigated whether Cbt requires E2F1 activity at all to delay cell cycle exit. In *Drosophila*, loss of *Dp* is believed to remove all E2F transcriptional activity, both activating and repressive, yet cells mutant for *Dp* cycle and exit the cell cycle relatively normally (20, 41). We used the MARCM system to generate *cbt* overexpressing cells that were also homozygous null for *Dp*, and analyzed these for ectopic mitoses. Clones were induced between 48 and 72 h AED and analyzed in pupal wings at 30 h APF. Ectopic mitoses were evident (Fig. 7 A–C). The ability of Cbt to drive ectopic proliferation in *Dp* mutant cells, which should lack both E2F activating and repressive activities, suggests that the Cbt-induced cell cycling does not require E2F1 activity. We also tested whether ectopic *cbt* could rescue the effects of loss of *E2f1* in proliferating wing cells. We used the MARCM system to generate GFP-labeled *E2f1* mutant clones that overexpressed *cbt* in imaginal wing discs at 72 h AED, and scored the number of

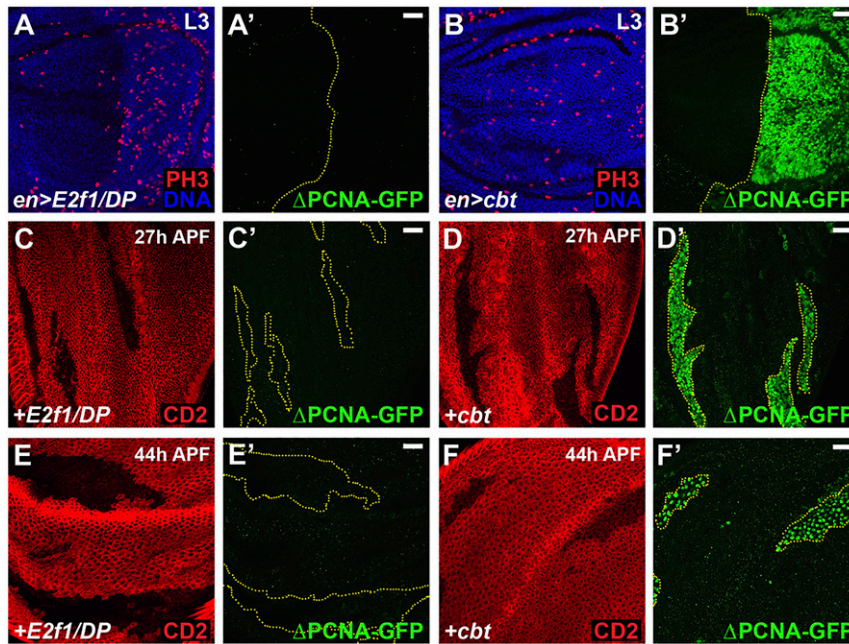


Fig. 6. Cbt activates the *PCNA-GFP* reporter independent of the E2F1 binding sites. (A and B) *en-Gal4* was used to express either *E2f1/DP* (A) or *cbt* (B) in the proliferating cells of third-instar wing discs. Mitoses were detected by anti-PH3 antibody staining (A and B) and expression of a *PCNA-GFP* reporter mutated in the E2F1 binding sites (Δ *PCNA-GFP*) was analyzed (A' and B'). Nuclei were stained with Hoechst (blue). (C–F) Clones marked by the absence of CD2 (red) expressing either *E2f1/DP* (C and E) or *cbt* (D and F) were induced at 48 to 72 h AED by the *hs-flp;act > CD2 > Gal4* and examined at the given times for Δ *PCNA-GFP* expression. *E2f1/DP* expression did not activate the Δ *PCNA-GFP* reporter at any time point (A, C, and E). Cbt strongly activated the Δ *PCNA-GFP* reporter at all time points (B, D, and F) (Scale bars, 20 μ m.)

cells per clone 48 h later. In this case, *cbt* overexpression did not rescue the cell cycle arrest that occurs in *E2f1*⁷¹⁷² mutant cells, whereas the overexpression of *E2f1/DP* complexes in these cells did rescue them (Fig. 7D). Cell cycle arrest in *E2f1* mutant cells is believed to result from an increase in E2F2- and Rbf-mediated transcriptional repression (32), which is evidently dominant to overexpressed *cbt*.

Discussion

For many years, it has been known that *Drosophila* cells lacking all E2F1 activating and repressive activity (*Dp* mutant or *e2f1/*

e2f2 double-mutant cells) can express cell cycle genes sufficiently to support extensive cell proliferation (32, 68, 69). Thus, despite the fact the E2Fs are by far the best-characterized and most-specific cell cycle regulatory transcription factors, there must be other transcription factors that can fill E2F1's role. In *Drosophila*, DREF has been proposed to be one such factor (70), and the DREAM complex also plays an important role, albeit in association with E2F/Dp and RB family factors (71). In this study we present the SP/KLF-like factor Cbt as a cell cycle regulatory transcription factor that has E2F1-like, but E2F1-independent, activity. Based on multiple lines of evidence, we propose that Cbt

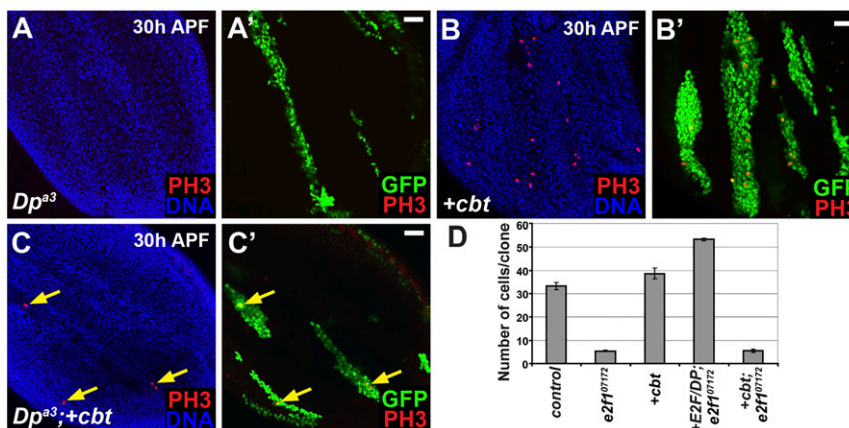


Fig. 7. Cbt does not require E2F1 activity to drive proliferation but cannot rescue the loss of *e2f1* (A–C) GFP⁺-labeled clones generated by the MARCM system at 48 to 72 h AED and analyzed at 30 h APF in pupal wings for ectopic mitoses by anti-PH3 staining (red). Nuclei were stained with Hoechst (blue). (A) Clones mutant for *Dp*^{a3-/-} did not undergo ectopic mitoses. (B) Ectopic mitoses were present in clones expressing *cbt*. (C) Clones mutant for *Dp*^{a3-/-} and expressing *cbt* also demonstrated ectopic mitoses (arrows). (D) Using the MARCM system GFP-labeled clones were induced at 72 h AED and number of cells per clone in wing discs was quantified 48 h later. There was no significant difference between *e2f1*⁷¹⁷² clones and *e2f1*⁷¹⁷² clones expressing *cbt*^{L^{A0930}}. (Scale bars, 20 μ m.)

activity directs the expression of cell cycle genes independently of both E2F1 activity and the E2F1 binding sites in the promoters of its targets. The ability of Cbt to activate its targets independently of E2F1 binding sites appears to lie in sequences in its N terminus, which are present only in the longer of the two Cbt protein isoforms expressed in *Drosophila* (SI Appendix, Figs. S2A and S6A). Interestingly, it is these N-terminal sequences that make Cbt more orthologous to human KLF10 and KLF11 than to other KLF genes (SI Appendix, Fig. S6A). Our findings suggest a model in which Cbt provides cells with an additional pathway by which they can control the transcription of cell cycle genes. By cross-comparing published Cbt ChIP-seq data (49) and E2F1 ChIP-chip data (72), we found a significant overlap ($P < 10^{-27}$, hypergeometric test) that 117 genes are mutual targets of both Cbt and E2F1 (SI Appendix, Table S5). GO analysis suggested that these 117 genes mediate a broad range of functions, including DNA replication, cell cycle, and multiple metabolic processes (SI Appendix, Table S6), further suggesting that Cbt is a critical cell cycle regulator that can complement E2F1 in many cellular contexts.

In the developing wing and eye the potent activity of E2F1 in proliferating cells appears to mask the ability of Cbt to regulate its cell cycle targets, but when E2F1 transcriptional activating activity is diminished, as occurs at cell cycle exit in the wing and eye discs, or at steady-state in the adult midgut, ectopic Cbt activity is capable of driving inappropriate cell cycles. Interestingly however, Cbt was not capable of promoting the expression of either CycE or Stg in the wing, the two factors previously shown to be proximal rate-limiting regulators of G1/S and G2/M progression in the developing fly wing and eye. Because of this, we propose that, in the pupal wing and eye, *cbt* overexpression may induce ectopic proliferation by providing higher than normal levels of a set of downstream genes that are required for DNA replication and mitosis (e.g., *Mcm5*, *-7*, *Orc2*, *-6*, *CycB3*, *fzy*) and that this increase in substrate availability permits residual CycE/Cdk2 and Stg/Cyclin/Cdk1 activity to drive additional S and M phases.

Beyond E2F1, another regulatory pathway that plays a fundamental role for cell cycle progression is the Hippo pathway. Yki, the downstream transcriptional activator of the Hippo pathway, controls multiple cell cycle regulators' expression (e.g., E2F1 and CycE) (73, 74). A previous study (49) proposed that Cbt associates with Yki to promote cell proliferation. Ruiz-Romero et al. (49) showed that Diap1-GFP, a Yki activity reporter, is decreased in *cbt* mutant (*dTIEG^{S14/S14}*) clones, suggesting that *cbt* is required for Yki activation. However, this conclusion is confounded by the fact that the *dTIEG^{S14}* allele used in that paper is a large deletion that removes the DNA encoding both *cbt* and *MED15*. We reexamined the regulation of Yki activity by Cbt using our *cbt^{D41}* allele, which doesn't impact *MED15*. In *cbt^{D41/D41}* mutant clones, the expression of the Yki target, Diap1, was normal (SI Appendix, Fig. S7A and A'). However, knockdown of *MED15* did significantly suppress the expression of Diap1 (SI Appendix, Fig. S7B and B'), indicating that the decrease in Diap1-GFP in *dTIEG^{S14}* mutant cells was due to the loss of *MED15* rather than *cbt*. Hence, we conclude that Cbt regulates cell proliferation independently of the Hippo pathway.

In mammals, the *cbt* homologs *KLF10* and *KLF11* are rapidly expressed following induction of TGF- β signaling, and interact with Smad family members to function as effectors of TGF- β signaling (42, 75–82). In this study, we identified a putative regulatory motif of GCAGYKGCAGCG that resembles a Mad-like motif (SI Appendix, Fig. S4C), consistent with the established relationship in both *Drosophila* and mammals between Cbt and the TGF- β signaling pathway (42, 45, 46, 83). Further work exploring the relationships between Cbt, E2F1, and the TGF- β signaling pathway may help elucidate an unsuspected relationship between this key developmental signaling pathway and cell cycle control.

The ability of Cbt to induce ectopic cell proliferation in the wing, eye, and gut suggests that it could have oncogenic function. Indeed, ectopic activity of several members of the SP/KLF family has been associated with a variety of cancerous phenotypes (84–88). Although the most immediate mammalian homologs of *cbt*, *KLF10* and *KLF11* (members of the TIEG family), are known primarily as cell cycle repressors (42), *KLF10* overexpression has nevertheless also been detected in several cancer cell lines, including renal clear cell carcinoma and glioblastoma (89). In these cancers, *KLF10* activity is thought to increase TGF- β signaling and thereby to promote adhesion, migration, and regeneration in epithelial cell types (89, 90). This is consistent with data showing that overexpression of *KLF10* in certain cell types has effects resembling those caused by activation of TGF- β signaling, and suggests a positive feedback loop between *KLF10* and TGF- β signaling (78, 79, 82, 91). Furthermore, when we refer to patient data from The Cancer Genome Atlas, we notice that among 220 colorectal adenocarcinoma patients with mutations and copy number variations, 9.5% of them have *KLF10* gene amplification or *KLF10* ectopic overexpression. This is in line with our oncogenic phenotype of Cbt in fly gut. Similarly, high *KLF11* expression has been associated with gastric and breast cancers (92, 93). How these connections might play out in terms of cell cycle control is an interesting topic for future studies.

Materials and Methods

Fly Strains. Please see SI Appendix, Supplementary Materials and Methods for details on fly strains.

Cbt Mutagenesis. A P-element insertion, *P[GawB]cbt[NP5201]* (Kyoto # 104895), resides in the first intron of the *cbt* gene. After the mobilization of *P[GawB]cbt[NP5201]* driven by $\Delta 2-3$ transposase, the *cbt* deletions were screened using the following primers: Fwd: TGGTTGCTCCACTGCCGATGACC; Rev: CCCTCATCAAGCAAAAAACATTCC.

Two mutants, *cbt^{D41}* and *cbt^{D148}*, were obtained from screening. Genomic PCR and subsequent sequencing showed that *cbt^{D41}* had a 900-bp deletion, which impaired the coding region of all three *cbt* transcript isoforms (RA, RB, and RC). *cbt^{D148}* had a 1,018-bp deletion, which deleted 59 bp of the first exon of *cbt*-RA but didn't alter the exons of *cbt*-RB or *cbt*-RC.

Generation of PCNA-miniwhite⁺ and GMR-Gal4(ey-CFP). The PCNA promoter was amplified from genomic DNA using the following primer pair: Fwd: CCCAAGCTTCCCAACACAGTTGGCAGGCCGC and Rev: CATGAATTCTGTGTTTATATATTAATACTGATGACG. The amplified PCR product was digested using HindIII and EcoRI and cloned into *pBlueScript II* HindIII/EcoRI sites. The resulting vector is *pBS-PCNA*. The *miniwhite⁺* gene was amplified from *pUAST* using the following primer pair: Fwd: CCGGAATTCATGGCCCAAGAGGATCAGGAG and Rev: AACTGCAGCCGAATTAATTCTAGTTCAG. The amplified PCR product was digested using EcoRI and PstI and cloned into *pBlueScript II* EcoRI/PstI sites. The resulting vector is *pBS-miniwhite⁺*. An EcoRI/PstI fragment from *pBS-miniwhite⁺* containing the *miniwhite⁺* coding sequence was cloned into EcoRI/PstI sites of *pBS-PCNA*. The resulting vector is *pBS-PCNA-miniwhite⁺*. *SmaI/XhoI* fragment from *pBS-PCNA-miniwhite⁺* containing *PCNA-miniwhite⁺* was cloned into the *piggyBac* vector *pBSII-ITR1.1k-ECFP* to generate *pBac.ECFP*. *PCNA-miniwhite⁺* *PiggyBac* transformants were generated by coinjecting *pBac.ECFP*. *PCNA-miniwhite⁺* with *pBSII-Act5c-orf* (*piggyBac* transposase). To generate *GMR-Gal4(ey-CFP)*, an *XhoI/HindIII* (blunted) fragment from *pGMR* containing *GMR*, *hsp70Bb* and *hsp70Ab* was cloned into the *XhoI/StuI* sites of *pBac.ECFP*, the resulting vector is *pBac-GMR.ECFP*. A *BglIII/BamHI* fragment from *pGMR-Gal4* containing the *Gal4* coding sequence was cloned into the *BglIII* site of *pBac-GMR.ECFP*, between *hsp70Ab* and *hsp70Ab* sequences, the resulting vector is *pBac-GMR-Gal4.ECFP*.

Immunostaining. Please see SI Appendix, Supplementary Materials and Methods for details on immunostaining.

Clonal Analysis. Overexpression clones were generated by either the heat-shock *hs-flip;act > CD2 > Gal4* method or the *hs-flip;tub > CD2 > Gal4* method with *tub-Gal80^{ts}* (51) inactivated at 29 °C. Hours APF represent equivalent time at 25 °C and adjusted appropriately as described in Buttitta et al. (5). Larvae were heat-shocked for 10 min at 37 °C between 48 and 72 h AED. Loss-of-function clones (or appropriate controls) were either generated by

mitotic recombination (94) or by MARCM (95). Larvae were heat-shocked for 45 min-1 h between 48 and 72 h AED, staged at white prepupae (if necessary), and dissected at the designated time point. For the MARCM clone assay performed in the midgut, 2- to 3-d-old female flies were heat-shocked for 20 min at 34 °C and dissected at the designated time point.

Clone Cell Counts. Please see *SI Appendix, Supplementary Materials and Methods* for details on cell counts.

Flow Cytometry. Dissociation of cells from staged and dissected larvae and pupae was performed as described in refs. 5, 63, and 96. Cell counts per experiment were ~20,000 except in tissues 44 h APF, which had cell counts ~10,000. Each experiment was performed at least three times and representative examples are shown. Experiments were performed on a Vantage2 cell sorter and analyzed using CellQuest (Becton-Dickinson).

Microarrays. Please see *SI Appendix, Supplementary Materials and Methods* for details on microarrays.

RT-qPCR. Please see *SI Appendix, Supplementary Materials and Methods* for details on RT-qPCR.

1. A. Vidal, A. Koff, Cell-cycle inhibitors: Three families united by a common cause. *Gene* **247**, 1–15 (2000).
2. F. Foijer, R. M. Wolthuis, V. Doodeman, R. H. Medema, H. te Riele, Mitogen requirement for cell cycle progression in the absence of pocket protein activity. *Cancer Cell* **8**, 455–466 (2005).
3. W. Du, N. Dyson, The role of RBF in the introduction of G1 regulation during *Drosophila* embryogenesis. *EMBO J.* **18**, 916–925 (1999).
4. B. R. Pennycook, A. R. Barr, Restriction point regulation at the crossroads between quiescence and cell proliferation. *FEBS Lett.*, 10.1002/1873-3468.13867 (2020).
5. L. A. Buttitta, A. J. Katzaroff, C. L. Perez, A. de la Cruz, B. A. Edgar, A double-assurance mechanism controls cell cycle exit upon terminal differentiation in *Drosophila*. *Dev. Cell* **12**, 631–643 (2007).
6. L. A. Buttitta, B. A. Edgar, Mechanisms controlling cell cycle exit upon terminal differentiation. *Curr. Opin. Cell Biol.* **19**, 697–704 (2007).
7. J. P. Miller, N. Yeh, A. Vidal, A. Koff, Interweaving the cell cycle machinery with cell differentiation. *Cell Cycle* **6**, 2932–2938 (2007).
8. S. van den Heuvel, N. J. Dyson, Conserved functions of the pRB and E2F families. *Nat. Rev. Mol. Cell Biol.* **9**, 713–724 (2008).
9. I. Onoyama, K. I. Nakayama, Fbxw7 in cell cycle exit and stem cell maintenance: Insight from gene-targeted mice. *Cell Cycle* **7**, 3307–3313 (2008).
10. L. C. Firth, N. E. Baker, Extracellular signals responsible for spatially regulated proliferation in the differentiating *Drosophila* eye. *Dev. Cell* **8**, 541–551 (2005).
11. D. Sun, L. Buttitta, States of G₀ and the proliferation-quiescence decision in cells, tissues and during development. *Int. J. Dev. Biol.* **61**, 357–366 (2017).
12. G. D. Grant, J. G. Cook, The temporal regulation of S phase proteins during G₁. *Adv. Exp. Med. Biol.* **1042**, 335–369 (2017).
13. Y. Ma, D. J. McKay, L. Buttitta, Changes in chromatin accessibility ensure robust cell cycle exit in terminally differentiated cells. *PLoS Biol.* **17**, e3000378 (2019).
14. T. H. Cheung, T. A. Rando, Molecular regulation of stem cell quiescence. *Nat. Rev. Mol. Cell Biol.* **14**, 329–340 (2013).
15. S. G. Swygert *et al.*, Condensin-dependent chromatin compaction represses transcription globally during quiescence. *Mol. Cell* **73**, 533–546.e4 (2019).
16. D. K. Dimova, O. Stevaux, M. V. Frolov, N. J. Dyson, Cell cycle-dependent and cell cycle-independent control of transcription by the *Drosophila* E2F/RB pathway. *Genes Dev.* **17**, 2308–2320 (2003).
17. O. Stevaux, N. J. Dyson, A revised picture of the E2F transcriptional network and RB function. *Curr. Opin. Cell Biol.* **14**, 684–691 (2002).
18. S. Ishida *et al.*, Role for E2F in control of both DNA replication and mitotic functions as revealed from DNA microarray analysis. *Mol. Cell Biol.* **21**, 4684–4699 (2001).
19. S. Polager, Y. Kalma, E. Berkovich, D. Ginsberg, E2Fs up-regulate expression of genes involved in DNA replication, DNA repair and mitosis. *Oncogene* **21**, 437–446 (2002).
20. L. A. Buttitta, A. J. Katzaroff, B. A. Edgar, A robust cell cycle control mechanism limits E2F-induced proliferation of terminally differentiated cells in vivo. *J. Cell Biol.* **189**, 981–996 (2010).
21. N. Dyson, The regulation of E2F by pRB-family proteins. *Genes Dev.* **12**, 2245–2262 (1998).
22. N. J. Dyson, RB1: A prototype tumor suppressor and an enigma. *Genes Dev.* **30**, 1492–1502 (2016).
23. W. Du, J. Pogoriler, Retinoblastoma family genes. *Oncogene* **25**, 5190–5200 (2006).
24. A. M. Narasimha *et al.*, Cyclin D activates the Rb tumor suppressor by monophosphorylation. *eLife* **3**, e02872 (2014).
25. C. J. Sherr, J. M. Roberts, CDK inhibitors: Positive and negative regulators of G1-phase progression. *Genes Dev.* **13**, 1501–1512 (1999).
26. T. Otto, P. Sicinski, Cell cycle proteins as promising targets in cancer therapy. *Nat. Rev. Cancer* **17**, 93–115 (2017).
27. D. K. Dimova, N. J. Dyson, The E2F transcriptional network: Old acquaintances with new faces. *Oncogene* **24**, 2810–2826 (2005).

Statistical Analysis. Statistical analyses were performed using the GraphPad Prism 8. Statistical significance (*P* values) of experiments were calculated by unpaired two-tailed Student's *t* test. Statistical significance was denoted as follows: nonsignificant (ns) *P* > 0.05, **P* < 0.05, ***P* < 0.01, ****P* < 0.001, and *****P* < 0.0001.

Data Availability. All study data are included in the article and *SI Appendix*.

ACKNOWLEDGMENTS. We thank Harene Venghatakrishnan for assistance with the experiments reported in *SI Appendix, Fig. S6 B–E'*; J. Merriam, N. Paricio, R. Duronio, S. Di Talia, X. Bi, and I. Rodriguez for flies and/or antibodies; the Fred Hutchinson Cancer Research Center Imaging, Array, and Flow Cytometry Facilities for help with data acquisition and array hybridizations; to J. Davison and M. Morgan for help with statistical analysis; and the Van Gilst Laboratory for use of their equipment. This work was supported by the Huntsman Cancer Foundation and the Center for Genomic Medicine/Utah Genome Project at the University of Utah, and National Institutes of Health Grants R01 GM070887, R01 GM124434, and P30 CA042014 (to B.A.E.). A.J.K. was supported by Developmental Biology Training Grant T32 HDO7183. L.A.B. was supported by Leukemia & Lymphoma Society Special Fellowship (LLS#3370-09) and NIH K99 GM086517.

28. W. Du, M. Vidal, J. E. Xie, N. Dyson, RBF, a novel RB-related gene that regulates E2F activity and interacts with cyclin E in *Drosophila*. *Genes Dev.* **10**, 1206–1218 (1996).
29. T. Sawado *et al.*, dE2F2, a novel E2F-family transcription factor in *Drosophila melanogaster*. *Biochem. Biophys. Res. Commun.* **251**, 409–415 (1998).
30. J. C. de Nooij, M. A. Letendre, I. K. Hariharan, A cyclin-dependent kinase inhibitor, Dacapo, is necessary for timely exit from the cell cycle during *Drosophila* embryogenesis. *Cell* **87**, 1237–1247 (1996).
31. R. J. Duronio, P. H. O'Farrell, Developmental control of the G1 to S transition in *Drosophila*: Cyclin E is a limiting downstream target of E2F. *Genes Dev.* **9**, 1456–1468 (1995).
32. M. V. Frolov *et al.*, Functional antagonism between E2F family members. *Genes Dev.* **15**, 2146–2160 (2001).
33. R. L. Finley Jr, B. J. Thomas, S. L. Zipursky, R. Brent, Isolation of *Drosophila* cyclin D, a protein expressed in the morphogenetic furrow before entry into S phase. *Proc. Natl. Acad. Sci. U.S.A.* **93**, 3011–3015 (1996).
34. J. A. Knoblich *et al.*, Cyclin E controls S phase progression and its down-regulation during *Drosophila* embryogenesis is required for the arrest of cell proliferation. *Cell* **77**, 107–120 (1994).
35. K. H. Moberg, D. W. Bell, D. C. Wahrer, D. A. Haber, I. K. Hariharan, Archipelago regulates Cyclin E levels in *Drosophila* and is mutated in human cancer cell lines. *Nature* **413**, 311–316 (2001).
36. M. E. Lane *et al.*, Dacapo, a cyclin-dependent kinase inhibitor, stops cell proliferation during *Drosophila* development. *Cell* **87**, 1225–1235 (1996).
37. M. Schubiger, J. Palka, Changing spatial patterns of DNA replication in the developing wing of *Drosophila*. *Dev. Biol.* **123**, 145–153 (1987).
38. M. Milán, S. Campuzano, A. Garcia-Bellido, Cell cycling and patterned cell proliferation in the *Drosophila* wing during metamorphosis. *Proc. Natl. Acad. Sci. U.S.A.* **93**, 11687–11692 (1996).
39. T. Wolff, D. Ready, "Pattern formation in the *Drosophila* retina" in *The Development of Drosophila Melanogaster*, M. Bate, A. Arias, Eds. (Cold Spring Harbor Press, Cold Spring Harbor, NY, 1993), pp. 1277–1326.
40. L. Weng, C. Zhu, J. Xu, W. Du, Critical role of active repression by E2F and Rb proteins in endoreplication during *Drosophila* development. *EMBO J.* **22**, 3865–3875 (2003).
41. M. V. Frolov, N. S. Moon, N. J. Dyson, dDP is needed for normal cell proliferation. *Mol. Cell Biol.* **25**, 3027–3039 (2005).
42. B. Spittau, K. Krieglstein, Klf10 and Klf11 as mediators of TGF-beta superfamily signaling. *Cell Tissue Res.* **347**, 65–72 (2012).
43. S. A. Thacker, P. C. Bonnette, R. J. Duronio, The contribution of E2F-regulated transcription to *Drosophila* PCNA gene function. *Curr. Biol.* **13**, 53–58 (2003).
44. H. Steller, V. Pirrotta, Expression of the *Drosophila* white gene under the control of the hsp70 heat shock promoter. *EMBO J.* **4**, 3765–3772 (1985).
45. I. Rodriguez, *Drosophila* TIEG is a modulator of different signalling pathways involved in wing patterning and cell proliferation. *PLoS One* **6**, e18418 (2011).
46. S. Muñoz-Descalzo, J. Terol, N. Paricio, Cabut, a C2H2 zinc finger transcription factor, is required during *Drosophila* dorsal closure downstream of JNK signaling. *Dev. Biol.* **287**, 168–179 (2005).
47. S. Muñoz-Descalzo, Y. Belacortu, N. Paricio, Identification and analysis of Cabut orthologs in invertebrates and vertebrates. *Dev. Genes Evol.* **217**, 289–298 (2007).
48. G. Suske, E. Bruford, S. Philipsen, Mammalian SP/KLF transcription factors: Bring in the family. *Genomics* **85**, 551–556 (2005).
49. M. Ruiz-Romero, E. Blanco, N. Paricio, F. Serras, M. Corominas, Cabut/dTIEG associates with the transcription factor Yorkie for growth control. *EMBO Rep.* **16**, 362–369 (2015).
50. O. Bartok *et al.*, The transcription factor Cabut coordinates energy metabolism and the circadian clock in response to sugar sensing. *EMBO J.* **34**, 1538–1553 (2015).
51. S. E. McGuire, G. Roman, R. L. Davis, Gene expression systems in *Drosophila*: A synthesis of time and space. *Trends Genet.* **20**, 384–391 (2004).

52. B. A. Edgar, P. H. O'Farrell, Genetic control of cell division patterns in the *Drosophila* embryo. *Cell* **57**, 177–187 (1989).
53. A. Kumagai, W. G. Dunphy, The cdc25 protein controls tyrosine dephosphorylation of the cdc2 protein in a cell-free system. *Cell* **64**, 903–914 (1991).
54. B. A. Edgar, P. H. O'Farrell, The three postblastoderm cell cycles of *Drosophila* embryogenesis are regulated in G2 by string. *Cell* **62**, 469–480 (1990).
55. T. Reis, B. A. Edgar, Negative regulation of dE2F1 by cyclin-dependent kinases controls cell cycle timing. *Cell* **117**, 253–264 (2004).
56. N. Zielke *et al.*, Fly-FUCCI: A versatile tool for studying cell proliferation in complex tissues. *Cell Rep.* **7**, 588–598 (2014).
57. Y. Jin *et al.*, EGFR/Ras signaling controls *Drosophila* intestinal stem cell proliferation via capicua-regulated genes. *PLoS Genet.* **11**, e1005634 (2015).
58. S. A. Blythe, E. F. Wieschaus, Establishment and maintenance of heritable chromatin structure during early *Drosophila* embryogenesis. *eLife* **5**, e20148 (2016).
59. R. B. Beckstead, G. Lam, C. S. Thummel, The genomic response to 20-hydroxyecdysone at the onset of *Drosophila* metamorphosis. *Genome Biol.* **6**, R99 (2005).
60. D. A. Guertin, K. V. Guntur, G. W. Bell, C. C. Thoreen, D. M. Sabatini, Functional genomics identifies TOR-regulated genes that control growth and division. *Curr. Biol.* **16**, 958–970 (2006).
61. S. Kadener, J. S. Menet, R. Schoer, M. Rosbash, Circadian transcription contributes to core period determination in *Drosophila*. *PLoS Biol.* **6**, e119 (2008).
62. R. Kraut, K. Menon, K. Zinn, A gain-of-function screen for genes controlling motor axon guidance and synaptogenesis in *Drosophila*. *Curr. Biol.* **11**, 417–430 (2001).
63. T. P. Neufeld, A. F. de la Cruz, L. A. Johnston, B. A. Edgar, Coordination of growth and cell division in the *Drosophila* wing. *Cell* **93**, 1183–1193 (1998).
64. R. J. Duronio, P. H. O'Farrell, J. E. Xie, A. Brook, N. Dyson, The transcription factor E2F is required for S phase during *Drosophila* embryogenesis. *Genes Dev.* **9**, 1445–1455 (1995).
65. A. Brook, J. E. Xie, W. Du, N. Dyson, Requirements for dE2F function in proliferating cells and in post-mitotic differentiating cells. *EMBO J.* **15**, 3676–3683 (1996).
66. M. Joe Song, C. C. Hong, Y. Zhang, L. Buttitta, B. A. Edgar, Comparative generalized logic modeling reveals differential gene interactions during cell cycle exit in *Drosophila* wing development. *Gl Ed. Proc.* **157**, 143–152 (2009).
67. S. E. Celniker *et al.*, modENCODE Consortium, Unlocking the secrets of the genome. *Nature* **459**, 927–930 (2009).
68. R. J. Duronio, P. C. Bonnette, P. H. O'Farrell, Mutations of the *Drosophila* dDP, dE2F, and cyclin E genes reveal distinct roles for the E2F-DP transcription factor and cyclin E during the G1-S transition. *Mol. Cell. Biol.* **18**, 141–151 (1998).
69. I. Royzman, A. J. Whittaker, T. L. Orr-Weaver, Mutations in *Drosophila* DP and E2F distinguish G1-S progression from an associated transcriptional program. *Genes Dev.* **11**, 1999–2011 (1997).
70. N. T. Tue *et al.*, DREF plays multiple roles during *Drosophila* development. *Biochim. Biophys. Acta. Gene Regul. Mech.* **1860**, 705–712 (2017).
71. S. Sadasivam, J. A. DeCaprio, The DREAM complex: Master coordinator of cell cycle-dependent gene expression. *Nat. Rev. Cancer* **13**, 585–595 (2013).
72. M. Korenjak, E. Anderssen, S. Ramaswamy, J. R. Whetstone, N. J. Dyson, RBF binding to both canonical E2F targets and noncanonical targets depends on functional dE2F/dDP complexes. *Mol. Cell. Biol.* **32**, 4375–4387 (2012).
73. N. Tapon *et al.*, Salvador promotes both cell cycle exit and apoptosis in *Drosophila* and is mutated in human cancer cell lines. *Cell* **110**, 467–478 (2002).
74. P. Zhang *et al.*, A balance of Yki/Sd activator and E2F1/Sd repressor complexes controls cell survival and affects organ size. *Dev. Cell* **43**, 603–617.e5 (2017).
75. M. Subramaniam *et al.*, Identification of a novel TGF-beta-regulated gene encoding a putative zinc finger protein in human osteoblasts. *Nucleic Acids Res.* **23**, 4907–4912 (1995).
76. T. Cook, R. Urrutia, TIEG proteins join the Smads as TGF-beta-regulated transcription factors that control pancreatic cell growth. *Am. J. Physiol. Gastrointest. Liver Physiol.* **278**, G513–G521 (2000).
77. T. Cook, B. Gebelein, K. Mesa, A. Mladek, R. Urrutia, Molecular cloning and characterization of TIEG2 reveals a new subfamily of transforming growth factor-beta-inducible Sp1-like zinc finger-encoding genes involved in the regulation of cell growth. *J. Biol. Chem.* **273**, 25929–25936 (1998).
78. I. Tachibana *et al.*, Overexpression of the TGFbeta-regulated zinc finger encoding gene, TIEG, induces apoptosis in pancreatic epithelial cells. *J. Clin. Invest.* **99**, 2365–2374 (1997).
79. M. Subramaniam, J. R. Hawse, S. A. Johnsen, T. C. Spelsberg, Role of TIEG1 in biological processes and disease states. *J. Cell. Biochem.* **102**, 539–548 (2007).
80. S. A. Johnsen, M. Subramaniam, T. Katagiri, R. Janknecht, T. C. Spelsberg, Transcriptional regulation of Smad2 is required for enhancement of TGFbeta/Smad signaling by TGFbeta inducible early gene. *J. Cell. Biochem.* **87**, 233–241 (2002).
81. S. A. Johnsen, M. Subramaniam, R. Janknecht, T. C. Spelsberg, TGFbeta inducible early gene enhances TGFbeta/Smad-dependent transcriptional responses. *Oncogene* **21**, 5783–5790 (2002).
82. V. Ellenrieder, TGFbeta regulated gene expression by Smads and Sp1/KLF-like transcription factors in cancer. *Anticancer Res.* **28**, 1531–1539 (2008).
83. J. M. Lee *et al.*, KLF10 is a modulatory factor of chondrocyte hypertrophy in developing skeleton. *J. Orthop. Res.* **38**, 1987–1995 (2020).
84. J. Kaczynski, T. Cook, R. Urrutia, Sp1- and Krüppel-like transcription factors. *Genome Biol.* **4**, 206 (2003).
85. C. Bureau *et al.*, Expression and function of Kruppel like-factors (KLF) in carcinogenesis. *Curr. Genomics* **10**, 353–360 (2009).
86. A. R. Black, J. D. Black, J. Azizkhan-Clifford, Sp1 and Krüppel-like factor family of transcription factors in cell growth regulation and cancer. *J. Cell. Physiol.* **188**, 143–160 (2001).
87. S. Safe, M. Abdelrahim, Sp transcription factor family and its role in cancer. *Eur. J. Cancer* **41**, 2438–2448 (2005).
88. A. Memon, W. K. Lee, KLF10 as a tumor suppressor gene and its TGF-β signaling. *Cancers (Basel)* **10**, 161 (2018).
89. S. V. Ivanov *et al.*, Two novel VHL targets, TGFBI (BIGH3) and its transactivator KLF10, are up-regulated in renal clear cell carcinoma and other tumors. *Biochem. Biophys. Res. Commun.* **370**, 536–540 (2008).
90. S. W. Park *et al.*, Beta ig-h3 promotes renal proximal tubular epithelial cell adhesion, migration and proliferation through the interaction with alpha3beta1 integrin. *Exp. Mol. Med.* **36**, 211–219 (2004).
91. T. E. Hefferan *et al.*, Overexpression of a nuclear protein, TIEG, mimics transforming growth factor-beta action in human osteoblast cells. *J. Biol. Chem.* **275**, 20255–20259 (2000).
92. Q. Ji *et al.*, KLF11 promotes gastric cancer invasion and migration by increasing Twist1 expression. *Neoplasia* **66**, 92–100 (2019).
93. L. Cheng, L. Shi, H. Dai, Bioinformatics analysis of potential prognostic biomarkers among Krüppel-like transcription factors (KLFs) in breast cancer. *Cancer Biomark.* **26**, 411–420 (2019).
94. T. Xu, G. M. Rubin, Analysis of genetic mosaics in developing and adult *Drosophila* tissues. *Development* **117**, 1223–1237 (1993).
95. T. Lee, L. Luo, Mosaic analysis with a repressible cell marker (MARCM) for *Drosophila* neural development. *Trends Neurosci.* **24**, 251–254 (2001).
96. A. F. de la Cruz, B. A. Edgar, Flow cytometric analysis of *Drosophila* cells. *Methods Mol. Biol.* **420**, 373–389 (2008).
97. K. J. Livak, T. D. Schmittgen, Analysis of relative gene expression data using real-time quantitative PCR and the 2-(Delta Delta C(T)) Method. *Methods* **25**, 402–408 (2001).